The effect of quantized ETF, grouping, and power allocation on non-orthogonal multiple accesses for wireless communication networks

Original Scientific Paper

Amir F. Banob
Faculty of Engineering
Mansoura University
marioneta_mero@yahoo.com

Fayez W. Zaki
Faculty of Engineering
Mansoura University
fwzaki2017@gmail.com

Mohammed M. Ashour
Faculty of Engineering
Mansoura University
mohmoh2@yahoo.com

Abstract *– Nonorthogonal multiple access (NOMA) is a significant technology in radio resource sharing and it has been recognized as a favorable method in fifth-generation (5G) wireless networks to meet the requirements of system capacity, service latency, and user connectivity. Many schemes for NOMA have been proposed in the last few years. such as transmitter linear spreading-based NOMA as a code domain, as well as a linear minimum mean square error (LMMSE), parallel interference cancellation (PIC), and serial interference cancellation (SIC) with power allocation and grouping as a power domain at the receiver side for uplink NOMA. This work aims to evaluate the performance of multiple types of linear spreading-based NOMA schemes. Simulations are achieved for the error-rate performance evaluation of these NOMA schemes, received signal after detection, and received signal and effect of every user on the other. Evaluating the performance of these technologies with comparison is also achieved through using grouping and power allocation. Simulations are achieved for the sum rate and spectral efficiency. For the future, 5G NOMA development, an equiangular tight frame (ETF) is suggested for improving performance and suggests grouping with 64qam-quantized Grassmannian for improving performance favorite about grouping with Generalized welch-bound equality (GWBE)*

Keywords*: Non-orthogonal multiple access (NOMA), fifth-generation (5G), equiangular tight frame (ETF), and generalized WBE (GWBE) sequences.*

1. INTRODUCTION

Non-orthogonal multiple access (NOMA) has been introduced for both uplink and downlink transmission schemes to provide the need for higher connectivity and data rate in wireless communications that participated in the development of 5G[1]. The power and code domains are the two major categories of NOMA schemes. Diverse power levels are allocated to users to permit interference cancellation at the receiver side, in the power domain NOMA[2]. The spreading-based NOMA techniques that are essential for the code domain can be accomplished by using sequence-based spreading [3],[4]. The commonly used receiver structure for symbol-based spreading is the parallel interference cancellation (PIC) receiver by uplink NOMA schemes, and grouping enhancement of multilevel average received powers can be combined with all existing NOMA schemes [5]. As part of the NOMA studies for 5G, several sequence-based spreading schemes are used, such as Grassmannian[6], [7], 64QAM-quantized Grassmannian[6], [7], pattern division multiple access (PCMA) [8], Welch-bound spreading multiple access (WSMA) [7], and generalized welch-bound equality (GWBE) sequences[7]. The spreading sequences with the lowest cross-correlation are supposed to be the preferable solution for NOMA transmission[9]. This work

aims to investigate and evaluate the performance of sequence-based spreading uplink NOMA for the above techniques compared with equiangular tight frame (ETF) matrix (4,8), and matrix (6,12) constructs by Paley's conference matrix. To gain further insight into spreading sequence design. The combination of power and code domain should be taken into consideration as well; more precisely, in addition to seeking sequences with low cross-correlations.

This paper is organized as follows: In Section II the system model provides 8 or 12 active detected users for six MA sequence spreading-NOMA as the code domain, and power allocation and grouping as the power domain are illustrated. Section III proposes strategies for NOMA improvements uplink performance. In section IV, the simulation results are presented.

2. LITERATURE REVIEW

To develop the mobile communication frameworks from the initial generation until 5G networks and beyond systems, many attempts have been developed to provide an increase in data rate requirements [10]. The recommendation of the International Telecommunication Union (ITU) for the IMT-2020 system, and the use of scripts for 5G and beyond frameworks included massive machine-type communications (mMTC), enhanced mobile broadband (eMBB), and reliable and self-contained communications Low latency (URLLC) [11]. Modern requirements become 1000 x average data rate for 4G with a response time of 1 ms, and 106 connections/km2[12]. With NOMA, users can be served with substantial resources such as frequency and/or time together with the use of sophisticated receivers. The 1st proposal of NOMA was to be applied to downlink to improve system capacity [13]. However, depending on the power variation among users, capabilities for uplink and downlink can grow by the NOMA field, which can achieve a 1.5x increase in system capacity [14]. Therefore, user association, energy allocation, and scheduling are studied extensively in many kinds of literature [15]. Various NOMA schemes, such as interleaved-division multiple access (IDMA), sparse code multiple access (SCMA) and multi-user shared access (MUSA) were introduced [16].In Release 14, other multiple access (MA) (such as sequences, codebook, mapping pattern and interleaved) are used to group doubled users and simplified multi-user detection (MUD) at the receiver [17]. Due to the limited time in Release 14, NOMA was not completed [18]. Release 15 focused on the uplink However, power is not hard done by Releases 14 or 15, which assumed equal power at the receiver without enhancing the performance by power difference, which is an important issue of uplink NOMA [10]. The trade-off between complexity and performance by sequence-based NOMA schemes was explained in [19]. There are a variety of topics in Release 16 studies, including Multimedia Priority Service, Vehicle-to-everything (V2X) application layer services, access to 5G satellites, support local area network in 5G, 5G wireless and wired convergence, terminal positioning and location, vertical domains communications and automation for network and techniques for novel radio [20].

3. SYSTEM MODEL

Some M users in uplink NOMA were spreading sequence (SS) vector s_k to the base station (BS), let b_M be the transmitted symbol that balances a unit norm. The additive white Gaussian noise (AWGN) signal model may be given as y=Sb+z, where z is the zero-mean AWGN vector with a covariance matrix I, i.e., an identity matrix. The in general SS matrix with an SS codeword (CW) in each of its columns is S, and the transmit symbol vector is b. It begins with the received power of each user being set to unity. A unit norm receives filter $f_{k'}$ such as a linear minimum mean squared error (MMSE) filter, which may be employed by the receiver to obtain an estimate $\hat{b}_k$ for the transmitted symbol b_k.[21]

$$y(t) = \sum_{k=1}^{M} \sqrt{P_M}\, h_M S_M(t) + n(t) \qquad (1)$$

Come from synchronization NOMA.

$$y(t) = \sum_{k=1}^{M} A_M\, b_M[i] S_M(t - iT - \tau_M) + n(t) \quad (2)\ [21]$$

where, $s(t)$ is the superposition of the data signals for the M-users each having different power, where T is the bit period, b_k {-1,1} is the information bit transmitted by user k during the time interval T, A_k is the amplitude of data received from user K, τ_k=0 for synchronization, $n(t)$ is the AWGN with unit power spectral density (which models the thermal noise and all other noise sources unrelated to the transmitted signals) and σ is the standard deviation of the noise. $\sigma 2$ variance. A_k=$\sqrt{P_{k'}}$ where h_i is the channel coefficient between m_{th} users and the base station (BS). [21]

Fig. 1. represents the transceiver uplink NOMA power domain

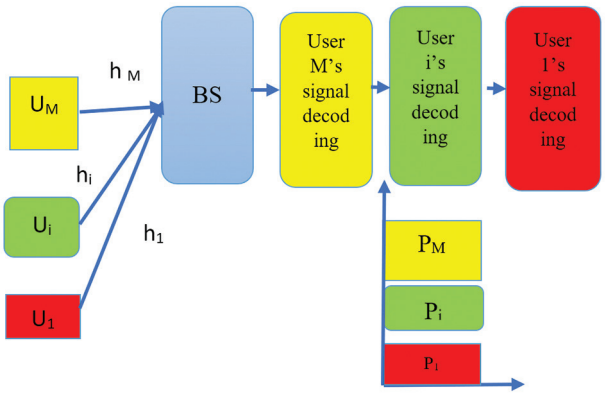

Fig. 1. transceiver uplink NOMA power domain

3.11 TRANSMITTER

3.1.1 MA SIGNATURES SEQUENCE

Comparing performance between six transmitted signals x_i has spreading-based NOMA schemes in 5G, namely, Grassmannian, 64QAM-quantized Grassmannian, PCMA, WSMA, GWBE, and ETF construct by Paley conference matrix. f_m is a unit norm receive filter, s_m is a unit norm spreading sequence (SS) vector, trace (.) represents the trace operator, v_m represents the noise component in the SINR γ_m, and w is the zero-mean AWGN vector with a covariance matrix I, i.e., an identity matrix, where s_m is employed by the receiver to obtain the estimation of the received signals. The postprocessing $SINR_m\gamma_m$ can be expressed as follows

$$\gamma_m = \frac{|f_m^H s_m|^2}{\sum_{i=1,i\neq m}^{M}|f_m^H s_m|^2 + |f_m^H w|^2} = \frac{f_m^H (s_m s_m^H) f_m}{f_m^H (\sum_{i=1,i\neq m}^{N} s_i s_i^H + I) f_m},$$
$$\xrightarrow{f_m = s_m} SINR_m = \frac{1}{trace\left((ss^T)^2\right) - 1 + v_m} \quad (3)\ [22]\ [23]$$

The trace(.) term in the denominator is the total squared correlation (TSC). If the postprocessing noise is white, the noise power of each v_m is the same. It is known that reducing the denominator or comparably increasing $SINR_m$, where TSC can be particularly used as a performance metric and it is expressed as follows: after $\sum_{l=1}^{m}\sum_{J=1}^{m}|S_l^H S_J|^2$ Let $R_m = (\sum_{i=1,\ i\neq m}^{m} s_i s_i^H + I)$ is the correlation matrix of the interference plus noise for the mth user, R_m it can be identified that minimizing the denominator or equivalently maximizing γ_m is a well-known Rayleigh-quotient problem [22][23]

Fig. 2. represents the NOMA transmitter

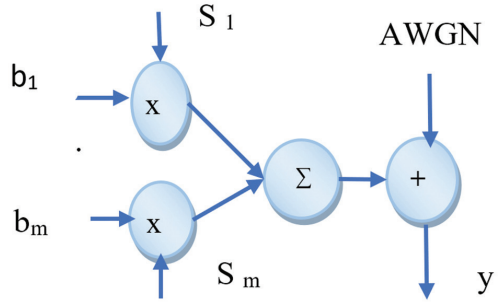

Fig. 2. NOMA transmitter

Sequence-based spreading NOMA schemes are considered 5G and rely on short-length sequences. Since the number of users is usually larger than the spreading factor, i.e., $N > K$, there will always be some cross-correlation among the sequences. Selecting the right codebook for a spreading-based NOMA is the key to achieving high performance, that is, the NOMA code domain

A finite unit-norm frame over the field C^m is a sequence of N vectors $fi \in C^m$; $1 \leq i \leq N$; that satisfies $\|fi_2\| = 1$ and $\alpha\|v\|_2^2 \leq \sum_{i=1}^{N} |f_i^H v|^2 \leq \beta\|v\|_2^2$, $\forall v \in C^m$. The paper introduces the frame synthesis matrix $F \in C^{m\times N}$ consisting of the concatenated frame vectors $F=[f1\ \ f2\ \ f3\ \ f4\ \ .....fN]$. Constants of $\alpha, \beta \in R\ with\ 0 < \alpha \leq \beta < \infty$ are called the lower and upper bounds of the frame. If $\alpha = \beta$ then the frame is called tight.

3.2. SPREADING-CODE NOMA SCHEMES IN 5G

In this section, six spreading-based NOMA schemes Grassmannian, 64QAM-quantized Grassmannian, PCMA, WSMA, and GWBE, compared with the constructing Equiangular tight frame (ETF) are investigated, and the sequence and quantized version of the sequence can be obtained as follows.

GRASSMANNIAN SEQUENCE [24]

The chordal Distance method supposes we have two k–dimensional subspaces S, T in $G(k,n)$, and the columns of S, $T \in R^{n\times k}$ form orthonormal bases for S, T, respectively. The chordal distance between S and T, as a function of (S,T), is given by

$$d_{chord}(S,T) = \sqrt{sin^2\theta_1 + \ldots + sin^2\theta_k} = [k - \|S \times T\|_F^2]^{\frac{1}{2}} \quad (4)$$

principal angles between S and T is $\{\theta 1,\ldots,\theta k\} \in [0,\pi/2]$. Based on the SVD decomposition, $S^T T = U\,\Sigma V^T$, $\Sigma ii = cos_{\theta i}$, $i \in [k]$, and the second equation comes from $\|S^T T\|_F^2 = \sum_{i=1}^{k} COS^2\,\theta_k$. Given the Grassmannian manifold $G(k,n)$ of k–dimensional subspaces of the real Euclidean n–dimensional space R^n, find a set of N k–dimensional subspaces $\{S1,\ldots,SN\} \subseteq G(k,n)$ spanned by the matrices $F = \{F1,\ldots,FN\}$, that solves the mathematical program

$$\max_{\mathcal{F}:\,|\mathcal{F}| = N} \ \min_{Fi,\,Fj \in \mathcal{F},\,i \neq j} \ d_{chord}(Fi, Fj) \quad (5)$$

64QAM-QUANTIZED GRASSMANNIAN [25]

Constrain by Grassmannian spreading codebooks are normalized by multiplying $P_{no,N,K}$, which is $(K\times K)$ normalized matrix for the power constraints,

$$P_{no,N,K} = \begin{bmatrix} P_{no,1} & 0 & 0 & 0 \\ 0 & P_{no,2} & 0 & 0 \\ 0 & 0 & \ddots & 0 \\ 0 & 0 & 0 & P_{no,K} \end{bmatrix}.$$

Here, $P_{no,N,K} = (1/|c^{(k)}|) \times \sqrt{N}$, for $k=1,\ldots,K$. quantized via coefficients from 64QAM modulation.

The mapping function for the 64-point modulated symbol sequence of length 2 is listed in table 1. The constellation of output symbols is shown in fig (3), where x can be either 0 or 1 which means four-bit sequences are mapped to the same symbol.

Table 1 Mapping function for the 64-point modulated symbol sequence of length 2 shows the relation between the corresponding bit sequence and output symbol sequence. This table explains how to construct the 64QAM-quantized Grassmannian from the Grassmannian spreading sequence.

Table 1. Mapping function for the 64-point modulated symbol sequence of length 2

000 000	000 001	000 010	000 011	000 100	000 101	000 110	000 111
$\begin{bmatrix}1+j\\1+j\end{bmatrix}$	$\begin{bmatrix}1+3j\\1+3j\end{bmatrix}$	$\begin{bmatrix}1-j\\1+j\end{bmatrix}$	$\begin{bmatrix}1-3j\\1+3j\end{bmatrix}$	$\begin{bmatrix}3+j\\3+j\end{bmatrix}$	$\begin{bmatrix}3+3j\\3+3j\end{bmatrix}$	$\begin{bmatrix}3-j\\3+j\end{bmatrix}$	$\begin{bmatrix}3-3j\\3+3j\end{bmatrix}$
001 000	001 001	001 010	001 011	001 100	001 101	001 110	001 111
$\begin{bmatrix}-1+j\\1+j\end{bmatrix}$	$\begin{bmatrix}-1+3j\\1+3j\end{bmatrix}$	$\begin{bmatrix}-1-j\\1+j\end{bmatrix}$	$\begin{bmatrix}-1-3j\\1+3j\end{bmatrix}$	$\begin{bmatrix}-3+j\\3+j\end{bmatrix}$	$\begin{bmatrix}-3+3j\\3+3j\end{bmatrix}$	$\begin{bmatrix}-3-j\\3+j\end{bmatrix}$	$\begin{bmatrix}-3-3j\\3+3j\end{bmatrix}$
010 000	010 001	010 010	010 011	010 100	010 101	010 110	010 111
$\begin{bmatrix}1+j\\1-j\end{bmatrix}$	$\begin{bmatrix}1+3j\\1-3j\end{bmatrix}$	$\begin{bmatrix}1-j\\1-j\end{bmatrix}$	$\begin{bmatrix}1-3j\\1-3j\end{bmatrix}$	$\begin{bmatrix}3+j\\3-j\end{bmatrix}$	$\begin{bmatrix}3+3j\\3-3j\end{bmatrix}$	$\begin{bmatrix}3-j\\3-j\end{bmatrix}$	$\begin{bmatrix}3-3j\\3-3j\end{bmatrix}$
011 000	011 001	011 010	011 011	011 100	011 101	011 110	011 111
$\begin{bmatrix}-1+j\\1-j\end{bmatrix}$	$\begin{bmatrix}-1+3j\\1-3j\end{bmatrix}$	$\begin{bmatrix}-1-j\\1-j\end{bmatrix}$	$\begin{bmatrix}-1-3j\\1-3j\end{bmatrix}$	$\begin{bmatrix}-3+j\\3-j\end{bmatrix}$	$\begin{bmatrix}-3+3j\\3-3j\end{bmatrix}$	$\begin{bmatrix}-3-j\\3-j\end{bmatrix}$	$\begin{bmatrix}-3-3j\\3-3j\end{bmatrix}$
100 000	100 001	100 010	100 011	100 100	100 101	100 110	100 111
$\begin{bmatrix}1+j\\-1+j\end{bmatrix}$	$\begin{bmatrix}1+3j\\-1+3j\end{bmatrix}$	$\begin{bmatrix}1-j\\-1+j\end{bmatrix}$	$\begin{bmatrix}1-3j\\-1+3j\end{bmatrix}$	$\begin{bmatrix}3+j\\-3+j\end{bmatrix}$	$\begin{bmatrix}3+3j\\-3+3j\end{bmatrix}$	$\begin{bmatrix}3-j\\-3+j\end{bmatrix}$	$\begin{bmatrix}3-3j\\-3+3j\end{bmatrix}$
101 000	101 001	101 010	101 011	101 100	101 101	101 110	101 111
$\begin{bmatrix}-1+j\\-1+j\end{bmatrix}$	$\begin{bmatrix}-1+3j\\-1+3j\end{bmatrix}$	$\begin{bmatrix}-1-j\\-1+j\end{bmatrix}$	$\begin{bmatrix}-1-3j\\-1+3j\end{bmatrix}$	$\begin{bmatrix}-3+j\\-3+j\end{bmatrix}$	$\begin{bmatrix}-3+3j\\-3+3j\end{bmatrix}$	$\begin{bmatrix}-3-j\\-3+j\end{bmatrix}$	$\begin{bmatrix}-3-3j\\-3+3j\end{bmatrix}$
110 000	110 001	110 010	110 011	110 100	110 101	110 110	110 111
$\begin{bmatrix}1+j\\-1-j\end{bmatrix}$	$\begin{bmatrix}1+3j\\-1-3j\end{bmatrix}$	$\begin{bmatrix}1-j\\-1-j\end{bmatrix}$	$\begin{bmatrix}1-3j\\-1-3j\end{bmatrix}$	$\begin{bmatrix}3+j\\-3-j\end{bmatrix}$	$\begin{bmatrix}3+3j\\-3-3j\end{bmatrix}$	$\begin{bmatrix}3-j\\-3-j\end{bmatrix}$	$\begin{bmatrix}3-3j\\-3-3j\end{bmatrix}$
111 000	111 001	111 010	111 011	111 100	111 101	111 110	111 111
$\begin{bmatrix}-1+j\\-1-j\end{bmatrix}$	$\begin{bmatrix}-1+3j\\-1-3j\end{bmatrix}$	$\begin{bmatrix}-1-j\\-1-j\end{bmatrix}$	$\begin{bmatrix}-1-3j\\-1-3j\end{bmatrix}$	$\begin{bmatrix}-3+j\\-3-j\end{bmatrix}$	$\begin{bmatrix}-3+3j\\-3-3j\end{bmatrix}$	$\begin{bmatrix}-3-j\\-3-j\end{bmatrix}$	$\begin{bmatrix}-3-3j\\-3-3j\end{bmatrix}$

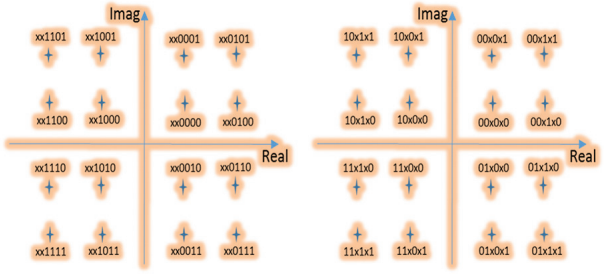

(a) RE1 (b) RE2

Fig. 3. 64 Point modulation constellation, x can be either 0 or 1.

PDMA [26] **TYPE OF SPARSE SEQUENCE.**

The transmitter side processing of PDMA with single-layer transmission is illustrated in Fig. 4. K users share the same time-frequency resources. For each UE, after channel coding and modulation, the modulated symbols are spread with a specific PDMA pattern, weighted by a given scaling factor, and then subjected to RE mapping. The details of the PDMA pattern, scaling factor, and RE mapping are given in the remainder of this section.

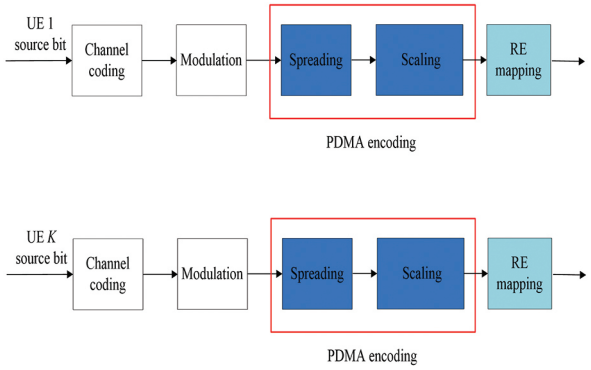

Fig. 4. PDMA with single-layer transmission

To support data transmission with higher spectral efficiency, PDMA with multiple-layer transmission can be supported. After channel coding and modulation, the modulated symbols are divided into multiple layers. For different layers, the modulated symbols are spread with different PDMA patterns separately, and then weighted by independent scaling factors. Then, data from different layers are summed up and subjected to RE mapping. The PDMA pattern defines the sparse symbol-level spreading sequence in Figure 4. PDMA pattern g_k is an N×1 binary vector with elements "0" and "1", where N denotes the spreading factor and "1" can also be replaced by complex values. The K users' a PDMA patterns construct the PDMA pattern matrix $G^{[N,K]}_{PDMA}$ with the dimension of $N \times K$:$G^{[N,K]}_{PDMA} = [g1, g2, \ldots, gk,]$. The scaling factor can be the power factor and/or phase factor. For PDMA with single-layer transmission, the scaling factor can be the power factor. $factor_{scaling}(K)$ for the PDMA pattern gk, which achieves normalizing each RE power to be 1, can be calculated as follows:

$$factor_{scaling}(k) = \sqrt{\frac{N}{sum(abs(g_k).\hat{}2)}} \tag{6}$$

For PDMA with multiple-layer transmission, the scaling factor can be both a power factor and a phase factor. The different PDMA patterns for a single UE should be orthogonal.

RE mapping is two types of PDMA: type 1) Localized, and type 2) distributed. where 4 PRB and g_2= [1 1 1 0]^T are assumed. Given a sufficiently large number of PRB and frequency selective channels with a large delay spread, distributed RE mapping can provide more frequency diversity than localized RE mapping.

WSMA [27]

The design metric for the signature vectors is the total squared cross-correlation $T_c \triangleq \sum_{i,j} |\boldsymbol{s}_i^H \boldsymbol{s}_j|^2$. The lower bound on the total squared cross-correlation of any set of K vectors of length N is $K^2/N \leq T_c$. The WBE sequences are designed to meet the bound on the total squared cross-correlations of the vector set with equality $B_{Welch} \triangleq K^2/N$.

GENERALIZED WBE (GWBE) SEQUENCES [28]

When $\sum_{k=1}^{K} P_K \geq N \cdot max\{P_1, P_2, \ldots, P_K\}$,the powers of multiple users are close enough and there are no oversized users; i.e., $K = \varphi$.

In this case, it reduces to $\lambda^* = \frac{\sum_i p_i}{N} 1_N$, and the optimal sequences satisfy $S^*P(S^*)^H = \frac{\sum_i p_i}{N} I_N$. It can be easily found that when $P_k = P\ f$ or $\forall\ k$, $P = PI_K$, the optimal sequences satisfy $S^*\ (S^*)^H = \frac{K}{N} I_N$ [10]

3.1.2.

To find the optimal power allocation for MA signatures NOMA which enhances performance. It is necessary to assign different powers to each user's signals in a realistic communication system. For unequal received powers, the cross-correlations become $R_m = S^H PS$, where P=diag{P_1,..., P_m} is a diagonal matrix, whose diagonal elements are the received powers of M users. Then, the optimal sequences satisfy

$$\min_{s_m^H s_m=1\,\forall k} R_m = \|\boldsymbol{S}^H \boldsymbol{P}\boldsymbol{S}\|_F^2 = \sum_{i=1}^{m}\sum_{j=1}^{m} P_i P_j \left|\boldsymbol{s}_i^H \boldsymbol{s}_j\right|^2 \quad (7)\ [29]$$

where P_j is the received power of user j. We use offset power between users =2 dB, 3 dB, 5 dB. From equation (7) using power allocation to enhance performance is a well-known Rayleigh quotient problem in equation (3).

Apply this method for 64QAM-quantized Grassmannian and GWBE.

It is a natural phenomenon, that a near-far effect exists in cellular networks. Applying the power allocation method for all MA signatures NOMA schemes are arranged to descend the detected users by calculating total squared correlation=$\sum_{I=1}^{m}\sum_{J=1}^{m}\left|S_I^H S_J\right|^2$ for every user. Then assuming that $\check{p}_1 \geq \check{p}_2 \geq \cdots \geq \check{p}_m$, there is a constant offset power between every user and the total power remains constant.

$$\frac{1}{m}\sum_{i=1}^{m} p_i = \frac{1}{m}\sum_{m=1}^{M} \check{p}_i = P \quad (8)$$

where equal power p_i=1, m= numbers of users, P=$p_i \times m$, offset power = 1 dB, 3 dB, 5 dB. $\check{p}i$ is the new power for every user after using the offset power. Then, we study the effect of the power allocation method on the performance of MA signature NOMA schemes.

3.1.3

The third sequence with grouping enhances performance. In grouping with power allocation: For any sequence pool with L sequences, the sequence pool can be divided into G groups for interference reduction and performance enhancement. Only the cross-correlations among sequences in groups with lower received powers matter. Therefore, the optimal sequences in a group g should satisfy [29].

$$\min_{s_m^H s_m=1\,\forall k} R_m = \min_{S_g} \sum_{m,n\geq g}\sum_{i\in\mathcal{K}_m}\sum_{j\in\mathcal{K}_n} \tilde{P}_m \tilde{P}_n \left|\boldsymbol{s}_i^H \boldsymbol{s}_j\right|^2 \quad (9)$$

where S_g is composed of sequences for group g, K_m and $\tilde{P}_m$ denote the set of sequence indices and average received power of group m, respectively, and $\tilde{P}_1 \geq \cdots \geq \tilde{P}_G$, we will use offset power between groups =5 dB. From equation (21) using grouping with power allocation to enhance performance is a well-known Rayleigh quotient problem which in equation (3)

To enhance performance, apply the grouping method for all MA signatures NOMA schemes, first arrange to descend the detected users by calculating total squared correlation=$\sum_{I=1}^{m}\sum_{J=1}^{m}\left|S_I^H S_J\right|^2$ for every user, then compose the number of groups from descending users then assume $\check{p}_{G1} \geq \check{p}_{G2} \geq \check{p}_{G3}$, there is a constant offset power between every group and the total power remains constant; where

$$\frac{1}{m}\sum_{i=1}^{m} p_i = \frac{1}{n}\sum_{G=1}^{G_L}\sum_{n=1}^{n} \check{p}_G = P \quad (10)$$

Where p_i=1, m=numbers of users, P=$p_i \times m$, n=number of users in the group= no of groups, offset power = 1 dB, 3 dB, 5 dB, and the low power was given with the low total squared correlation group. The first trial divides users into two groups.

Fig. 5. represents the grouping method FIG (5) represents the grouping method apply this method for Grassmannian sequence, WSMA spreading, 64 QAM-quantized Grassmannian sequences, GWBE sequences, sparse sequences, and ETFs.

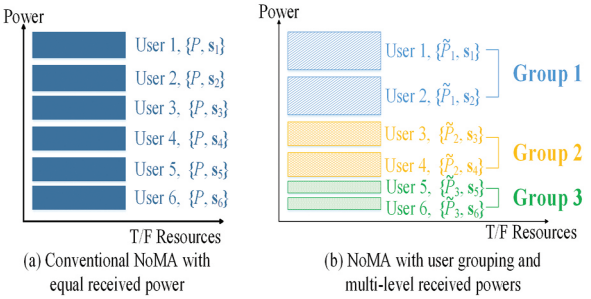

Fig. 5. grouping method

3.3 RECEIVER DETECTOR

Linear minimum mean square error (LMMSE), interference cancellation (parallel and serial) PIC, SIC.

Fig. 6. represents linear minimum mean square error (LMMSE)

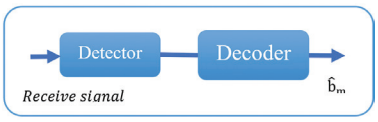

Fig. 6. Linear minimum mean square error (LMMSE)

$$\hat{b}_m = \operatorname{sgn}\left(\frac{1}{A_m}([R+\sigma^2 A^{-2}]^{-1} y)_m\right) = \operatorname{sgn}(([R+\sigma^2 A^{-2}]y)_m) \quad (11)\ [21]$$

Where R is normalized cross correlation, A is received amplitudes, and σ is the noise

PARALLEL INTERFERENCE CANCELLATION (PIC)

Fig (7) represents parallel interference cancellation (PIC)

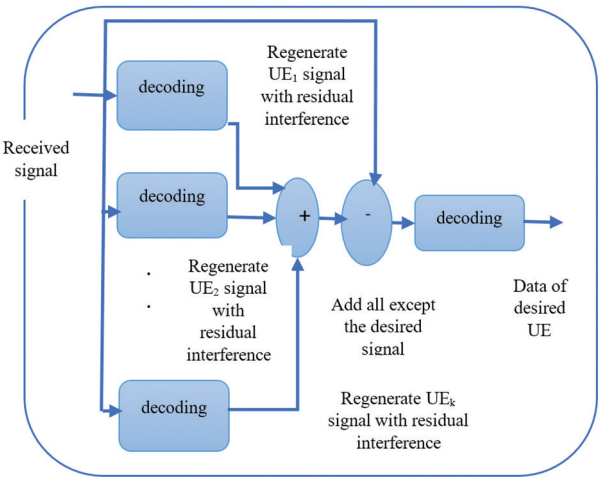

Fig. 7. Parallel interference cancellation (PIC)

An index n represents the iteration n=0, 1, 2, ..., the user (m=1, 2, ..., M), Let the symbol estimate $\hat{x}_m^{\,n}$. Those estimates from iteration n, updated estimate at iteration n+1 is

$$\hat{x}^{(n+1)} - A^{-1}\left(y - (\mathrm{R}-\mathrm{I})A\hat{X}^{(n)}\right) \quad (12)\ [30]$$

SERIAL INTERFERENCE CANCELLATION (SIC)

Let the strictly lower triangular part be L of R=L +L^t +I. Then the vector form is Estimates $\hat{x}^{(n)}$, and received vector y.

$$\hat{\mathrm{x}}^{\mathrm{n}+1} - \mathrm{A}^{-1}\left(\mathrm{y} - \mathrm{LA}\hat{\mathrm{x}}^{(\mathrm{n}-1)} - \mathrm{L}^{\mathrm{t}}\mathrm{A}\hat{\mathrm{x}}^{(\mathrm{n})}\right) \quad (13)\ [30]$$

Fig. 8. represents serial interference cancellation (SIC)

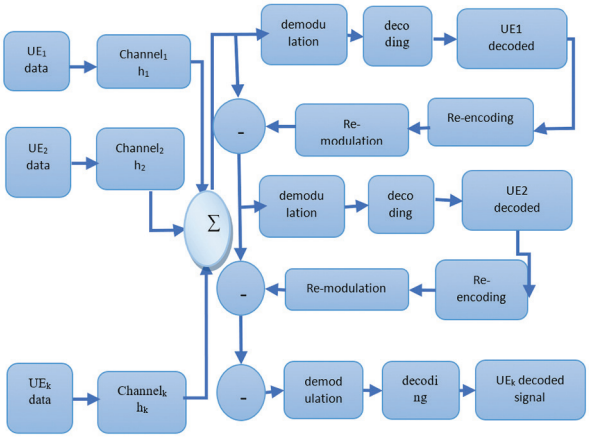

Fig. 8. Serial interference cancellation (SIC)

LINEAR MINIMUM MEAN SQUARE ERROR (LMMSE), PARALLEL INTERFERENCE CANCELLATION (PIC).

Fig (9) represents linear minimum mean square error (LMMSE) with parallel interference cancellation (PIC).

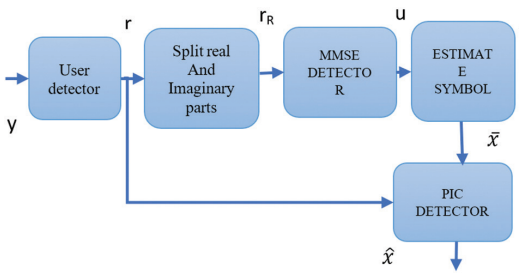

Fig. 9. Linear minimum mean square error (LMMSE) with parallel interference cancellation (PIC).

3.4 MATCHING BETWEEN ANALYTIC AND SIMULATION [31]

The corresponding general analytic synchronization bit error rate in NOMA for MF was calculated as the follows:

$$\mathrm{p_{em}} = \frac{1}{2^{\mathrm{N}-1}}\sum_{\mathrm{N}-1} Q\left(\frac{\mathrm{Am} + \sum \mathrm{Aj}\rho_{1\mathrm{j}}}{\sigma}\right) + Q\left(\frac{\mathrm{Am} - \sum \mathrm{Aj}\rho_{1\mathrm{j}}}{\sigma}\right) \quad ,\mathrm{j} \neq \mathrm{m} \qquad (14)$$

where ρ is the cross correlation, p is probability of error, A is received amplitudes and σ is the noise

$$\mathrm{real}(\rho_{\mathrm{ij}})\mathrm{used}, \mathrm{imaginary}(\rho_{\mathrm{ij}}) = 0, \mathrm{also\ neglects\ the\ first\ part}$$
$$0 \leq |\rho 1 \pm \rho_{12} \pm \rho_{13} \pm \rho_{14} \pm \rho_{15} \pm \rho_{16} \pm \rho_{17} \pm \rho_{18}| \leq 1$$

The corresponding general analytic synchronization bit error rate in NOMA for the correlator was calculated as the follows:

$$\mathrm{p_{em}} = \frac{1}{2^{\mathrm{N}-1}}\sum_{\substack{\mathrm{N}-1 \\ \mathrm{j} \neq \mathrm{m}}} Q\left(\frac{1 + \sum \mathrm{Aj}\rho_{1\mathrm{j}}}{\sigma}\right) + Q\left(\frac{1 - \sum \mathrm{Aj}\rho_{1\mathrm{j}}}{\sigma}\right), \quad (15)$$

$$\mathrm{real}(\rho_{\mathrm{ij}})\mathrm{used}, \mathrm{imaginary}(\rho_{\mathrm{ij}}) = 0, \mathrm{also\ neglects\ the\ first\ part}$$

3.5. ACHIEVABLE SUM-RATE ANALYSIS

For comparison among different CD NOMA schemes. evaluate in this section the achievable rates and the spectral efficiency. Compute the capacities of the continuous-input-continuous-output memoryless channel (CCMC)

3.5.1. CCMC CAPACITY

As a result, the ergodic CCMC capacity at the j-th user for the described NOMA system is generally (regardless of the employed scheme ETF, GWBE, PDMA, 64QAM-quantized Grassmannian, Grassmannian, and WSMA where SNR= JN_0, $\frac{J}{K}$=$frame\ gain$, k is the width dimension of the frame, $E_{H_{j,F}}$ is ergodic capacity, and N_0 is the spectral power density at each j receiver given by[32]

$$C_j^{CCMC} = E_{H_{j,F}}\left[log_2 \det\left(I_K + \frac{1}{JN_0} H_j F F^H H_j^H\right)\right] \quad (16)$$

The instances of the matrix F and the channel H_j greatly, influence the sum-rate performance.

4. PROPOSED NONORTHOGONAL MULTIPLE ACCESS (NOMA) ENHANCES UPLINK PERFORMANCE

In this section, three enhancements for uplink NOMA are proposed. The first at transmitter constrain ETF matrix (4,8), matrix (6,12) by Paley's conference matrix, where this transmitted matrix enhances performance compared with Grassmannian sequence, WSMA spreading, 64 QAM-quantized Grassmannian Sequence, GWBE sequences, and sparse sequence. The second proposed using power allocation with grouping to achieve the best performance for 64 QAM-quantized Grassmannian sequence, and GWBE sequences better than using only power allocation. The third proposed using grouping with 64QAM-quantized Grassmannian with a power offset of 5 dB enhances performance more than using grouping with GWBE with a power offset of 5 dB.

4.1 CONSTRUCT ETF MATRIX (4,8), AND MATRIX (6,12) BY PALEY'S CONFERENCE MATRIX ENHANCE PERFORMANCE COMPARE WITH USING POWER ALLOCATION OR GROUPING WITH POWER ALLOCATION FOR THESE MATRICES (GRASSMANNIAN SEQUENCE, WSMA SPREADING, 64 QAM-QUANTIZED GRASSMANNIAN SEQUENCE, GWBE SEQUENCES, AND PDMA SEQUENCE)

ETF for construction Conference matrix of size $n \times n$, Let ψ be a quadratic character of F. For different matrix $x, y \in F$ we write $Q = (\psi(x - y))$, The diagonal elements of Q are all 0 and the other elements are in {1,-1}. The matrix Q satisfies, $Q^{\top} = \begin{cases} Q \; if \; q \equiv 1 \; (mod \; 4) \\ -Q \; if \; q \equiv 3 \; (mod \; 4) \end{cases}$

conference matrix 8X8

$$\begin{bmatrix} 0 & +1 & +1 & +1 & +1 & +1 & +1 & +1 \\ -1 & 0 & +1 & +1 & -1 & +1 & -1 & -1 \\ -1 & -1 & 0 & +1 & +1 & -1 & +1 & -1 \\ -1 & -1 & -1 & 0 & +1 & +1 & -1 & +1 \\ -1 & +1 & -1 & -1 & 0 & +1 & +1 & -1 \\ -1 & -1 & +1 & -1 & -1 & 0 & +1 & +1 \\ -1 & +1 & -1 & +1 & -1 & -1 & 0 & +1 \\ -1 & +1 & +1 & -1 & +1 & -1 & -1 & 0 \end{bmatrix},$$

S (4x8)

$$\begin{bmatrix} -0.00 - 0.00\mathrm{i} & 0.30 - 0.78\mathrm{i} & 0.07 + 0.20\mathrm{i} & 0.28 + 0.10\mathrm{i} \\ -0.20 - 0.26\mathrm{i} & 0.53 + 0.49\mathrm{i} & -0.38 + 0.16\mathrm{i} & -0.60 + 0.10\mathrm{i}, \ldots \\ \vdots & & & \\ -0.00 - 0.00\mathrm{i} & -0.16 - 0.10\mathrm{i} & -0.03 + 0.23\mathrm{i} & 0.22 - 0.67\mathrm{i} \\ 0.29 + 0.59\mathrm{i} & 0.03 + 0.27\mathrm{i} & -0.80 - 0.08\mathrm{i} & 0.46 - 0.25\mathrm{i}, . . \\ \vdots & & & \\ 0.00 - 0.00\mathrm{i} & 0.27 - 0.22\mathrm{i} & 0.57 + 0.65\mathrm{i} & -0.41 + 0.33\mathrm{i} \\ -0.54 + 0.16\mathrm{i} & -0.01 - 0.51\mathrm{i} & -0.20 - 0.06\mathrm{i} & 0.31 - 0.35\mathrm{i}, \ldots \\ \vdots & & & \\ -1.00 - 0.00\mathrm{i} & 0.00 - 0.38\mathrm{i} & -0.00 - 0.38\mathrm{i} & -0.00 - 0.38\mathrm{i} \\ -0.00 - 0.38\mathrm{i} & -0.00 - 0.38\mathrm{i} & -0.00 - 0.38\mathrm{i} & -0.00 - 0.38\mathrm{i} \end{bmatrix}$$

conference matrix12x12

$$\begin{bmatrix} 0 & +1 & +1 & +1 & +1 & +1 & +1 & +1 & +1 & +1 & +1 & +1 \\ -1 & 0 & +1 & -1 & +1 & +1 & +1 & -1 & -1 & -1 & +1 & -1 \\ -1 & -1 & 0 & +1 & -1 & +1 & +1 & +1 & -1 & -1 & -1 & +1 \\ -1 & +1 & -1 & 0 & +1 & -1 & +1 & +1 & +1 & -1 & -1 & -1 \\ -1 & -1 & +1 & -1 & 0 & +1 & -1 & +1 & +1 & +1 & -1 & -1 \\ -1 & -1 & -1 & +1 & -1 & 0 & +1 & -1 & +1 & +1 & +1 & -1 \\ -1 & -1 & -1 & -1 & +1 & -1 & 0 & +1 & -1 & +1 & +1 & +1 \\ -1 & +1 & -1 & -1 & -1 & +1 & -1 & 0 & +1 & -1 & +1 & +1 \\ -1 & +1 & +1 & -1 & -1 & -1 & +1 & -1 & 0 & +1 & -1 & +1 \\ -1 & +1 & +1 & +1 & -1 & -1 & -1 & +1 & -1 & 0 & +1 & -1 \\ -1 & -1 & +1 & +1 & +1 & -1 & -1 & -1 & +1 & -1 & 0 & +1 \\ -1 & +1 & -1 & +1 & +1 & +1 & -1 & -1 & -1 & +1 & -1 & 0 \end{bmatrix}$$

S (6X12)

$$\begin{bmatrix} -0.00 + 0.00\mathrm{i} & -0.034 - 0.01i & 0.18 + 0.60i & -0.08 - 0.05i \\ 0.45 - 0.17i & -0.52 + 0.14i & -0.39 - 0.45i & 0.21 + 0.33i \\ -0.10 + 0.19\mathrm{i} & 0.28 - 0.44\mathrm{i} & 0.31 - 0.18\mathrm{i} & -0.31 + 0.03\mathrm{i}, \ldots \\ \vdots & & & \\ 0.00 + 0.00\mathrm{i} & -0.017 + 0.017\mathrm{i} & -0.41 + 0.09\mathrm{i} & 0.04 - 0.48\mathrm{i} \\ 0.52 + 0.30i & -0.13 + 0.15i & -0.07 - 0.11i & -0.01 - 0.30i \\ 0.36 + 0.40\mathrm{i} & -0.58 + 0.37\mathrm{i} & 0.06 - 0.47\mathrm{i} & 0.22 + 0.02\mathrm{i}, \ldots \\ \vdots & & & \\ -0.00 + 0.00\mathrm{i} & 0.15 + 0.02\mathrm{i} & 0.30 + 0.05i & 0.38 - 0.46\mathrm{i} \\ 0.01 + 0.17i & -0.47 - 0.19i & 0.39 + 0.49i & -0.22 + 0.51i \\ 0.25 - 0.32\mathrm{i} & -0.13 - 0.13\mathrm{i} & -0.34 - 0.27\mathrm{i} & -0.32 + 0.14\mathrm{i}, \ldots \\ \vdots & & & \\ -1.00 - 0.00\mathrm{i} & 0.00 - 0.30\mathrm{i} & 0.00 - 0.30\mathrm{i} & 0.00 - 0.30\mathrm{i} \\ -0.00 - 0.30\mathrm{i} & 0.00 - 0.30\mathrm{i} & 0.00 - 0.30\mathrm{i} & 0.00 - 0.30\mathrm{i} \\ -0.00 - 0.30\mathrm{i} & -0.00 - 0.30\mathrm{i} & -0.00 - 0.30\mathrm{i} & -0.00 - 0.30\mathrm{i} \ldots \\ \vdots & & & \\ 0.00 - 0.00\mathrm{i} & -0.14 + 0.16\mathrm{i} & -0.12 + 0.23\mathrm{i} & -0.35 - 0.15\mathrm{i} \\ -0.43 - 0.19i & -0.20 - 0.46i & 0.19 - 0.07i & 0.20 - 0.35i \\ 0.61 - 0.07\mathrm{i} & 0.04 + 0.02\mathrm{i} & 0.36 + 0.17\mathrm{i} & -0.16 + 0.70\mathrm{i}, \ldots \\ \vdots & & & \\ -0.00 - 0.00\mathrm{i} & 0.87 - 0.27\mathrm{i} & -0.09 + 0.40\mathrm{i} & -0.26 - 0.27\mathrm{i} \\ -0.05 + 0.22i & 0.08 + 0.24i & -0.07 + 0.29i & -0.09 - 0.42i \\ -0.07 - 0.13\mathrm{i} & -0.17 - 0.28\mathrm{i} & 0.14 + 0.42\mathrm{i} & -0.28 - 0.19\mathrm{i} \end{bmatrix}$$

ii) $Qe = 0$,$QJ = 0$, iii) $QQ^{T} = qI - J$, where J is the matrix with all entries 1.$M = \begin{bmatrix} 0 & \boldsymbol{e}^{\top} \\ \psi(-1)\boldsymbol{e} & Q \end{bmatrix}$, the conference matrix created by Paley different sets SVD for the conference matrix to construct the complex matrix size $n \times n$, extract a tight frame from C via SVD size $n \times k$ by nonzero eigenvalues are the first d elements on the diagonal of V, then $fk = \frac{\sqrt{N}}{\sqrt{d}}\{V\mathrm{k}, \mathrm{l}\}_{l=1}^{d}, P$ for $k = 1, \ldots, N$ form an ETF in this example $\sqrt{2}$.

Let $\mathbf{R}_k = (\sum_{j=1,\ j\neq k}^{K} \mathbf{s}_j \mathbf{s}_j^H + \mathbf{I})$, which is the correlation matrix of the interference plus noise $\sum_{j=1, j\neq k}^{K} \mathbf{s}_j \mathbf{s}_j^H$

For (4,8), the maximum cross-correlation is different for each sequence: Grassmannian 0.5772, WSMA 0.6845; 64QAM-quantized Grassmannian 0.7217; GWBE sequences 0.7502; sparse spreading 0.8165, ETF= 0.3780 and R_k ETF=16, GWBE=17.2060, Grassmannian=18.047, WSMA=18.165, 64QAM-quantized Grassmannian=19.19, and sparse=22. For (6,12), the maximum cross-correlation is different for each sequence; Grassmannian 0.3904; WSMA 0.7027; 64QAM-quantized Grassmannian 0.5459, and ETF= 0.3015, ETF achieve less maximum cross-correlation ρ and R_k ETF=24, 64QAM-quantized Grassmannian=29.104, and Grassmannian=29.5231, ETF achieve less R_k .

4.2. PROPOSES GROUPING [4,4] FOR MA SIGNATURE WITH A POWER OFF SET BETTER THAN ONLY POWER ALLOCATION

Where *equation(9)* obtain enhance than for *equation(7)*

For our example with Grouping [4,4] with offset 5 dB mathematical calculation for R_x to 64QAM-quantized Grassmannian=16.8615, GWBE=17.068, 64QAM-quantized Grassmannian, R_x for 0 dB =`19.19, for 2 dB =19.757, for 3 dB =19.975, for 5 dB =20.2668, For GWBE, R_x for 0 dB =`17.206, for 2 dB =17.367, for 3 dB =17.450, for 5 dB =17.538

Notice that grouping enhances performance more than only using power location between users where power allocation does not give tangible enhancement in performance

4.3. PROPOSES GROUPING [4,4] WITH OFFSET POWER FOR 64QAM-QUANTIZED GRASSMANNIAN ENHANCES PERFORMANCE COMPARED TO GWBE

Grouping with Power allocation division of the 8 users into two groups [4, 4], power = 5 dB, LMMSE-PIC detector the optimal sequences in group g should satisfy *equation(9)* for all other types of MA signatures. ETF=16.758, 64QAM-quantized Grassmannian=16.8615, GWBE=17.068, Grassmannian=17.247, WSMA=17.356, and sparse=18.0908.

5. SIMULATION RESULTS AND DISCUSSION

In this section, we display our assessment of different sequence-based spreading NOMA schemes, namely, Grassmannian, 64QAM-quantized Grassmannian, PCMA, WSMA, GWBE, and ETF. The detailed simulation assumptions are provided in table (2), using MATLAB in simulations.

Table 2. Simulation parameters

Parameter	Value or assumption
Programming	MATLAB
Modulation	BPSK
Signature allocation	Fixed
Channel estimation	Ideal
Number of B.S antenna	1
Frame length (N)	4,6
Number of users(K)	8, 12, 16, 24,64
Offset power	1 dB, 3 dB, 5 dB
Interference cancelation	PIC, SIC
Noise	AWGN
S/N	0:2:18 dB
Receiver type	LMMSE-PIC

5.1 ON THE EFFECT OF SPREADING CODE SEQUENCES ON AVERAGE BER

comparison between analytic and simulation to 8 users for matched filter and correlator

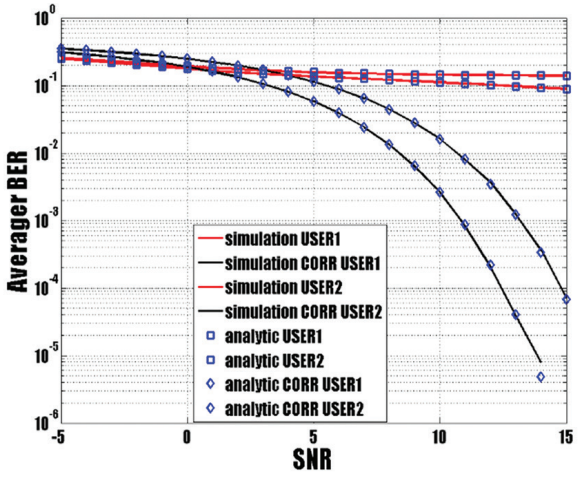

Fig. 10. GWBE spreading sequence relation between Average BER and SNR, Number of users =2

Fig (10) shows the relation between the average BER and SNR, where the number of users =2. A comparison between the analysis and simulation was carried out to ensure the used equations. The GWBE spreading sequence signal was applied using the MF detector and the correlation detector; there was a match between the analysis and simulation. The corresponding general analytic synchronization bit error rate in NOMA for MF was calculated as the follows.

Fig. (11,12,13,14,15) represent the BER versus the signal-to-noise ratio (SNR)

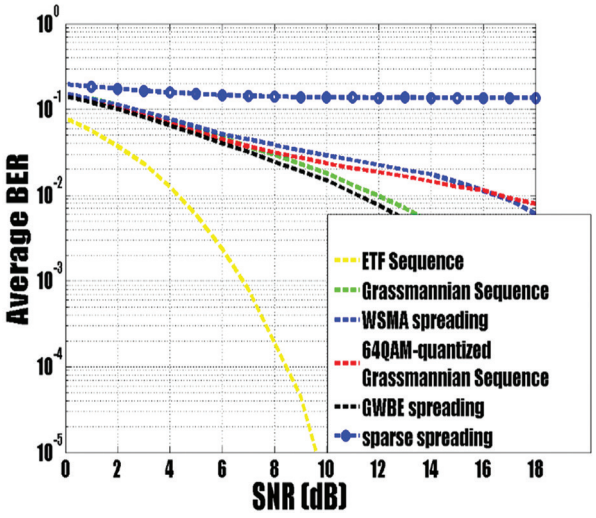

Fig. 11. Comparing the performance between different types of transmitted signals N=4

As shown in fig (11), where ETF NOMA spreading code where N=4, K=8, Grassmannian N=4, K=12, WSMA N=4, K=12, 64QAM-quantized Grassmannian N=4, K= 24, GWBE sequences N=4, K=16, PCMA K=64. assuming power for all users unity, receiver type is LMMSE-PIC, where $R= (\sum_{i=1,\ i\neq n}^{N} s_i s_i^H + I)$, compare the values of R for ETF=16, GWBE=17.2060, Grassmannian=18.047, WSMA=18.165, 64QAM-quantized Grassmannian=19.19, and sparse=22, by MATLAB simulation find that SNR will be enhanced for ETF than GWBE with gain in detection all 8 users and gain in performance, the figure shown that GWBE best than all other sequences which compact with 3GPP which considered GWBE sequence as a candidate for MA SIGNATURE sequence. Therefore, minimize the denominator $R = (\sum_{i=1,\ i\neq n}^{N} s_i s_i^H + I)$or equivalently maximize $SINR_m$.

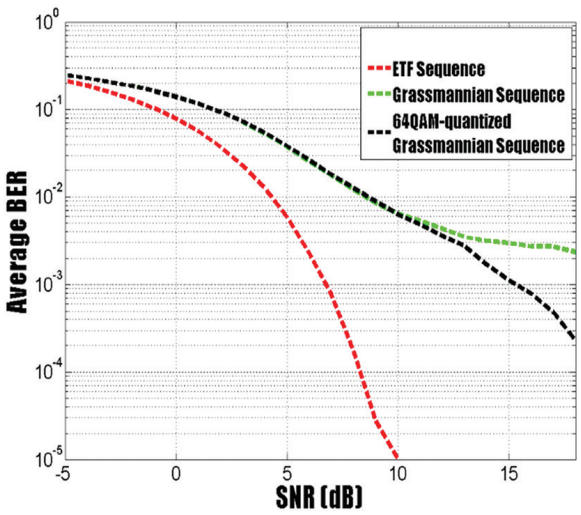

Fig. 12. Comparison between the performances of different types of transmitted signals N=6

Fig (12), where ETF NOMA spreading code N=6, K=12 for, Grassmannian N=6, K=24, 64QAM-quantized Grassmannian N=6, K= 24, detection for 12 users, with equal power, In figure 9 Calculate the value $R = (\sum_{i=1,\ i\neq n}^{N} s_i s_i^H + I)$ for ETF, Grassmannian, and 64QAM-quantized Grassmannian, ETF=24, 64QAM-quantized Grassmannian=29.104, and Grassmannian=29.5231, MATLAB simulation finds that SNR will be enhanced for ETF than 64QAM-quantized Grassmannian or Grassmannian. This figure confirms equation (3) where minimizing the denominator maximizes $SINR_n$, and proves the idea performance enhancement with ETF compared to other MA SIGNATURE sequences.

Fig. 11, and 12 illustrate that ETF spreading code enhancement performance gains 8 dB more than any other MA signature. Additionally, GWBE was better than all other sequences with 3GPP, which considered the GWBE sequence as a candidate for MA SIGNATURE sequence. This result was achieved by mathematic calculation and MATLAB simulation.

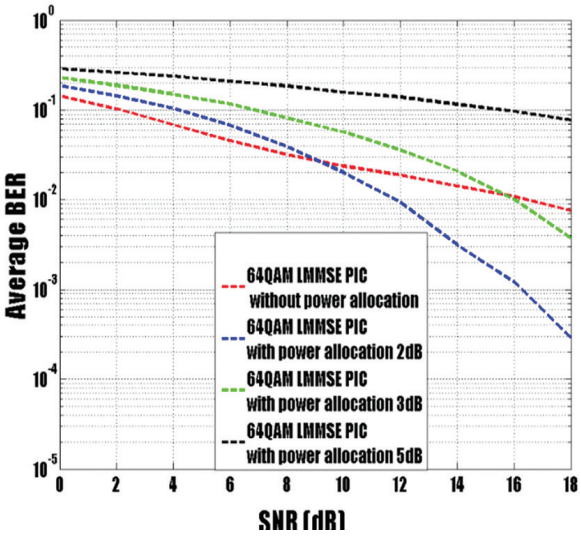

Fig. 13. Power allocation for 64QAM the spreading sequence code signal with offset power between users

Fig. 13 presents a try to obtain the optimal power allocation, where transmitted signal 64QAM spreading sequence code, where N=4 and k=24, detector LMMSE-PIC, detection for 8 users with different power offset between users =0 dB, 2 dB, 3 dB, and 5 dB. By mathematical calculation for *equation(8)* $\min_{s_k^H s_k=1\ \forall k} R_x = \|\boldsymbol{S}^H \boldsymbol{P}\boldsymbol{S}\|_F^2 = i{=}1Kj{=}1KPiPj\boldsymbol{s}iH\boldsymbol{s}j2, Rx$ for 0 dB =`19.19, for 2 dB =19.757, for 3 dB =19.975, for 5 dB =20.2668, compact with MATLAB simulation, shows that the best BER performance at 0 dB, then BER performance goes from bad to worse when using power allocation with power offset between users = 2 dB, 3 dB, and 5 dB for 64QAM-quantized Grassmannian spreading sequence code.

Fig. 14 presents attempt to obtain the optimal power allocation, transmitted signal GWBE spreading sequence code, where N=4 and k=16, detector LMMSE-PIC, detection for 8 users with different power offsets between users =0 dB, 2 dB, 3 dB, and 5 dB. Then, by mathematical calculation for equation(7), R_x for 0 dB =`17.206, for 2 dB =17.367, for 3 dB =17.450, for 5 dB =17.538, compact with the MATLAB simulation where the best BER performance at 0 dB, the BER deteriorates when using power allocation with power offset between users = 2 dB, 3 dB, and 5 dB. for GWBE spreading sequence code.

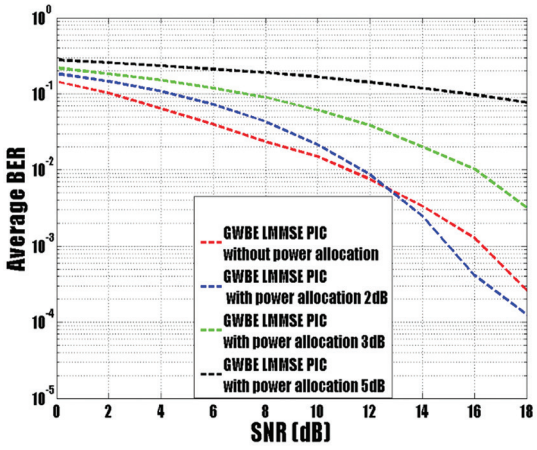

Fig. 14. Power allocation for THE GWBE spreading sequence code signal with offset power between users

Fig. 13, and 14 prove that $\min_{s_k^H s_k=1\ \forall k} R_x = \|\boldsymbol{S}^H \boldsymbol{P}\boldsymbol{S}\|_F^2 = \sum_{i=1}^{K}\sum_{j=1}^{K} P_i P_j \left|\boldsymbol{s}_i^H \boldsymbol{s}_j\right|^2$ is the controller for optimal sequences using power allocation for the MA SIGNATURE sequence.

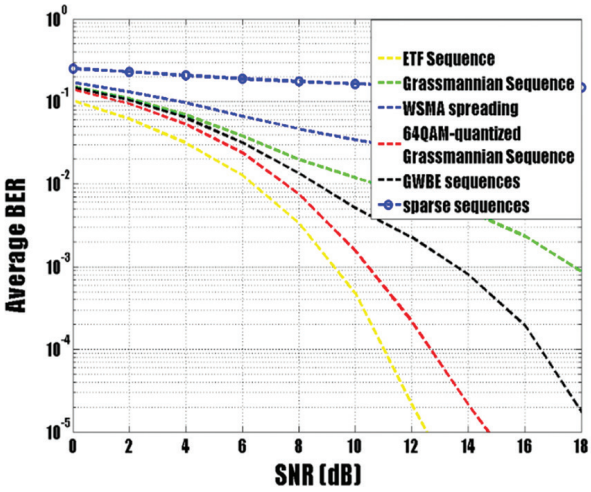

Fig. 15. Comparing the performance of different transmitted signals with grouping

Fig. 15. compares the performance of the transmitted signals (Grassmannian sequence N=4, k=12, WSMA spreading N=4, k=12, 64 QAM-quantized Grassmannian Sequence N=4, k=24, GWBE sequences N=4, k=16, and sparse sequence N=4, k=64) with a division of the 8 users into two groups [4, 4], power = 5 dB, LMMSE-

PIC detector the optimal sequences in group g should satisfy *equation(9)*, the mathematical calculation for R_x to ETF=16.758, 64QAM-quantized Grassmannian=16.8615, GWBE=17.068, Grassmannian=17.247, WSMA=17.356, and sparse=18.0908. Comparing these values with mathematical calculation ETF=16, GWBE=17.2060, Grassmannian=18.047, WSMA=18.165, 64QAM-quantized Grassmannian=19.19, and PCMA =22 in figure 4, we observe that grouping for GWBE with power allocation enhances performance more than without grouping, which agrees with 3GPP, which assumes that grouping for GWBE is a candidate for enhanced performance for MA SIGNATURE. Additionally, from a comparison for 64QAM-quantized Grassmannian, we conclude that grouping of 64QAM-quantized Grassmannian enhances performance more than without grouping, grouping for 64QAM-quantized Grassmannian enhances performance more than GWBE grouping, and ETF grouping still gives better performance than grouping for 64QAM-quantized Grassmannian and GWBE grouping. These results achieved by mathematic calculation and MATLAB simulation. Also comparing results for figure 8 with results for figure 6 which mathematical values R_x for 0 dB =`19.19, for 2 dB =19.757, for 3 dB =19.975, for 5 dB =20.2668 for 64QAM-quantized Grassmannian and with results for figure 12 which mathematical values $R_x$ for 0 dB =`17.206, for 2 dB =17.367, for 3 dB =17.450, for 5 dB =17.538 for GWBE. From the comparison, it can be concluded that grouping enhances performance more than without grouping or with only power allocation.

5.2 ON THE EFFECT OF SPREADING CODES ON THE RECEIVED SIGNAL AFTER DETECTION

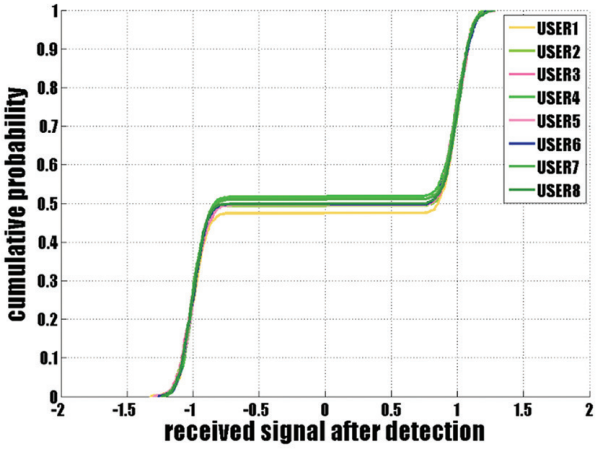

Fig. 16. CDF for ETF NOMA code

Fig. 16. illustrates detection for the ETF signal, detection for 8 users randomly with equal received power, where N=4, K=8, the empirical CDF presents in y-axis straight line increases begin near 1 and end near -1 for all 8 users mean that all users have received well after detection.

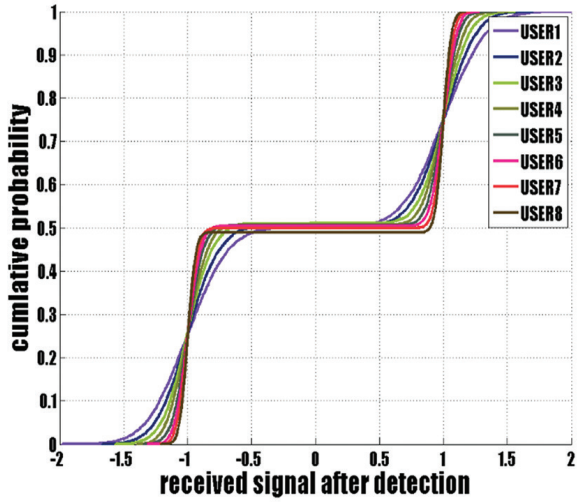

Fig. 17. CDF for GWBE NOMA code.

Fig. 17 shows the CDF for the GWBE spreading sequence, 8 users randomly received equal power. It illustrates that some users have straight-line increases beginning near 1 and ending near -1, and others have the straight line beginning near 0.5 and ending near -0.5, that is mean some users have received good detection, and others do not. The detection for all users is not similar; some are not perfect like the others

Compare figs (16,) and (17) by cumulative distribution function for 8 active users detected, which have been sent by ETF and GWBE NOMA spreading sequence, ETF better-received signal after detection than GWBE.

5.3 ON THE EFFECT OF SPREADING CODES ON THE RECEIVED SIGNAL AND THE EFFECT OF EVERY USER ON THE OTHER

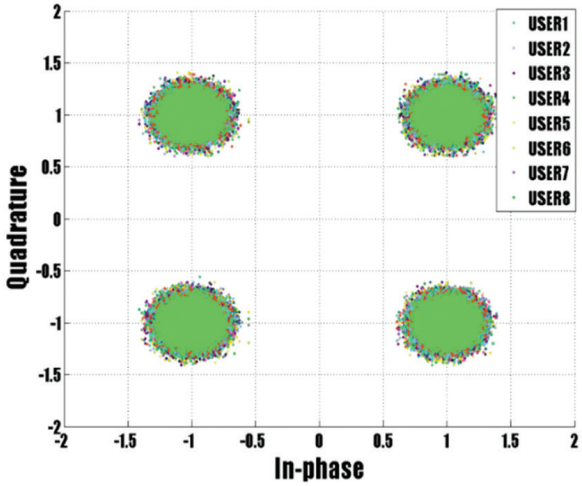

Fig. 18. Scatter diagram (constellation diagram), ETF NOMA spreading code

Fig (18) shows constellation diagrams for ETF sequence signals where N=4, K=8, and there are 8 users to detect. In MATLAB code we display the relation be-

tween any two users randomly, so here $\frac{k(k-1)}{2}$ relations among all users in the x-y plane (quadrature and in-phase). This reveals that the amount of data was more concentrated at approximately -1, -1. which means that the inter-symbol interference (ISI) is not too high.

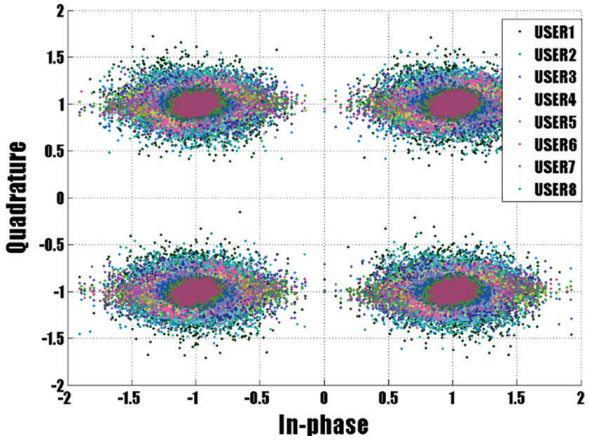

Fig. 19. Scatter diagram (constellation diagram), GWBE spreading code.

Fig (19) shows constellation diagrams for the GWBE sequence signal where N=4, K=8, and there are 8 users to detect with equal received power. In MATLAB code, we display the relation between any two users randomly, so here $\frac{k(k-1)}{2}$ relations among all users in the x-y plane (quadrature and in-phase). The data got dispersed far away from approximately (-1, 1), which means that there is inter-symbol interference (ISI) between users for GWBE transmitted signal.

Figs (18,) and (19) illustrate that GWBE clouds in the constellation have a higher spreading tendency than ETF, which causes higher performance degradation that illustrates ETF's better performance than GWBE. Constellation diagrams could be considered one of the major performance metrics for the NOMA design in NR.

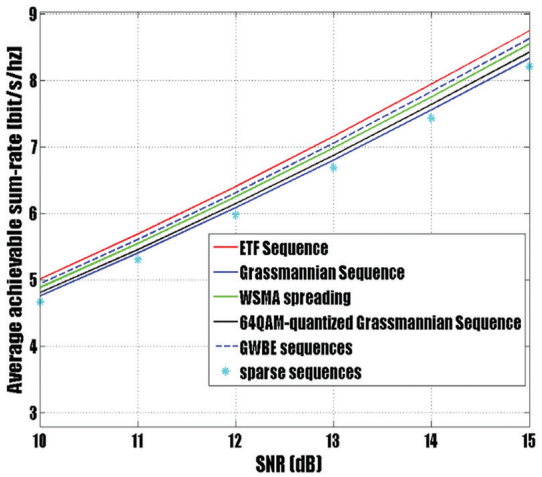

Fig. 20. CCMC capacity between ETF, GWBE, Grassmannian, WSMA, 64QAM-quantized Grassmannian, and sparse with j=4, K=8

Fig. 20 shows the CCMC capacity for ETF, GWBE, Grassmannian, WSMA, 64QAM-quantized Grassmannian, and sparse. The results indicate that ETF obtains a higher spectrally normalized sum rate than the other NOMA schemes.

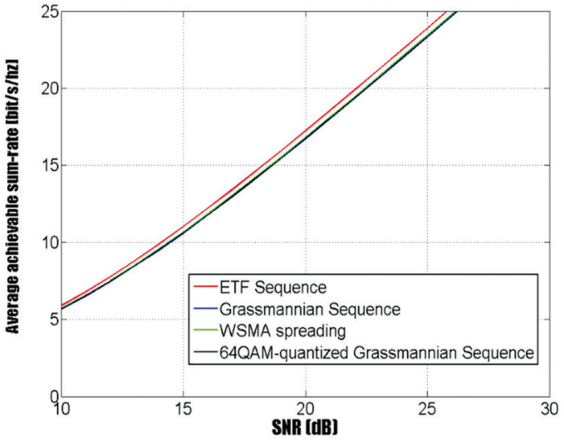

Fig. 21. CCMC capacity between ETF, Grassmannian, WSMA, and 64QAM-quantized Grassmannian with j=6, K=12

Fig (21) simulation shows the CCMC capacity for ETF, Grassmannian, WSMA, and 64QAM-quantized Grassmannian. The results indicate that ETF obtains a higher spectrally normalized sum rate than the other NOMA schemes

6. CONCLUSION

ETF enhances performance more than the Grassmannian sequence, WSMA spreading, 64 QAM-quantized Grassmannian sequence, GWBE sequence, and PDMA sequence, proving that by the effect of spreading code sequences on average BER, the effect of spreading codes on the received signal after detection and the effect of spreading codes on received signal and the effect of every user on the other. Grouping enhances performance more than using power allocation. 64 QAM-quantized Grassmannian sequence with grouping is better than GWBE sequences with grouping for enhancement performance. Simulation for the continuous-input-continuous-output memoryless channel capacity proves that ETF is optimal in achieving sum rates compared to other NOMA schemes

7. REFERENCE

[1] Z. Ding, M. Peng, H. V. Poor, "Cooperative non-orthogonal multiple access in 5G systems", IEEE Communications Letters, Vol. 19, No. 8, 2015, pp. 1462-1465.

[2] Z. Yang, Z. Ding, P. Fan, N. Al-Dhahir, "A general power allocation scheme to guarantee quality of service in downlink and uplink NOMA systems",

IEEE Transactions on Wireless Communications, Vol. 15, No. 11, 2016, pp. 7244-7257.

[3] 3GPP R1-1805840, "Key processing modules at transmitter side for NOMA, ZTE, RAN1 #93."

[4] 3GPP R1-1809434, "Transmitter Side Signal Processing Schemes for NOMA", Qualcomm Incorporated, RAN1 #94.

[5] 3GPP R1-1809148, "Transmitter design for uplink NOMA, Gothenburg, Sweden", TSG RAN WG1 Meeting #94.

[6] 3GPP R1-1808499, "Transmitter side signal processing schemes for NCMA", TSG RAN WG1 Meeting #94."

[7] 3GPP R1-1809844, "Email discussion to collect detailed description of the NOMA schemes", TSG RAN WG1 Meeting #94."

[8] 3GPP R1-1808386, "NOMA transmitter side signal processing", TSG RAN WG1 Meeting #94."

[9] J. H. Mott, "An algebraic method for the construction of families of sequences with good Hamming cross-correlation properties", Proceedings of the Twentieth Southeastern Symposium on System Theory, 1988, pp. 328-329.

[10] W. Liu, X. Hou, L. Chen, "Enhanced uplink non-orthogonal multiple access for 5G and beyond systems", Frontiers of Information Technology & Electronic Engineering, Vol. 19, No. 3, 2018, pp. 340-356.

[11] I. M. T. Vision, "Framework and overall objectives of the future development of IMT for 2020 and beyond", Radiocommunication Study Groups, 2015.

[12] J. G. Andrews et al. "What will 5G be?", IEEE Journal on Selected Areas in Communications, Vol. 32, No. 6, 2014, pp. 1065-1082.

[13] Y. Saito, Y. Kishiyama, A. Benjebbour, T. Nakamura, A. Li, K. Higuchi, "Non-orthogonal multiple access (NOMA) for cellular future radio access", Proceedings of the IEEE 77th vehicular technology conference, Dresden, Germany, 2-5 June 2013, pp. 1-5.

[14] D. Lopez-Perez et al. "A Survey on 5G Energy Efficiency: Massive MIMO, Lean Carrier Design, Sleep Modes, Machine Learning", arXiv2101.11246, 2021.

[15] X. Chen, A. Benjebbour, A. Li, A. Harada, "Multi-user proportional fair scheduling for uplink non-orthogonal multiple access (NOMA)", Proceedings of the IEEE 79th Vehicular Technology Conference, Seoul, Korea, 18-21 May 2014, pp. 1-5.

[16] Z. Yang, Z. Ding, P. Fan, G. K. Karagiannidis, "On the performance of non-orthogonal multiple access systems with partial channel information", IEEE Transactions on Communications, Vol. 64, No. 2, 2015, pp. 654-667.

[17] 3GPP T R 38.802, "Study on new radio access technology physical layer aspects." 3GPP Valbonne, France, 2017.

[18] A. Hoglund et al. "Overview of 3GPP release 14 enhanced NB-IoT", IEEE Netwetworks, Vol. 31, No. 6, 2017, pp. 16-22.

[19] R. Ratasuk, N. Mangalvedhe, Z. Xiong, M. Robert, D. Bhatoolaul, "Enhancements of narrowband IoT in 3GPP Rel-14 and Rel-15", Proceedings of the IEEE Conference on Standards for Communications and Networking, Helsinki, Finland, 18-20 September 2017, pp. 60-65.

[20] T.-K. Le, U. Salim, F. Kaltenberger, "An overview of physical layer design for Ultra-Reliable Low-Latency Communications in 3GPP Release 15, 16, 17", IEEE Access, Vol. 9, 2020. pp. 433-444.

[21] S. Halunga fratu, O. Fratu, "MULTIUSER DETECTION ALGORITHMS", 2005.

[22] K. Long, D. Chen, S. Duan, P. Wang, F. Wu, "Improved uplink NOMA performance through adaptive weighted factors aided PIC and MA signature", IEEE Access, Vol. 7, 2019, pp. 35908-35918.

[23] 3GPP R1-1806241, "Signature design for NoMABusan", TSG-RAN WG1 Meeting #93.

[24] T. Zheng, J. Guthrie, E. Mallada, "Inner Approximations of the Positive-Semidefinite Cone via Grassmannian Packings", arXiv2105.12021, 2021.

[25] 3GPP R1-1808151, "Transmitter side designs for NOMA", 3GPP TSG RAN WG1 Meeting #94."

[26] 3GPP R1-1808386, "NOMA transmitter side signal processing", TSG RAN WG1 Meeting #94.

[27] R.-1806241 3GPP, "Signature design for NoMA", Ericsson, RAN1#93.

[28] "3GPP TR 38.812., "' Study on Non-Orthogonal Multiple Access (NOMA) for NR"

[29] 2018v1. 3GPP, "Transmitter design for uplink NOMA", Technical Report R1-1809148, 2018."

[30] M. L. Honig, "Advances in multiuser detection", John Wiley & Sons, 2009.

[31] S. Verdu, "Multiuser detection. Cambridge university press, 1998.

[32] Hara, Takanori, et al. "On the Sum-Rate Capacity and Spectral Efficiency Gains of Massively Concurrent NOMA Systems", Proceedings of the IEEE Wireless Communications and Networking Conference, Marrakesh, Morocco, 15-18 April 2019.